Engineering Structures, 25(6), pp.801-8016, 2003

Control of Cable Vibrations Using Secondary Cable with Special Reference to Nonlinearity and Interaction

H. Yamaguchi* and Md. Alauddin[#]

Department of Civil and Environmental Engineering, Saitama University, 255 Shimo-Ohkubo, Saitama, 338-8570, Japan

[#] At present, Hyder Consulting, Sydney, Australia

*Corresponding author: Professor Hiroki Yamaguchi
Department of Civil and Environmental Engineering
Saitama University
255 Shimo-Ohkubo, Saitama, 338-8570, Japan

Phone: +81-48-858-3552
Fax: +81-48-858-3552

Email: hiroki@post.saitama-u.ac.jp

Abstract

Experimental as well as analytical studies have been carried out on the controlling effects of secondary cable in a cable system and efforts have been made to explain the results, especially on the basis of nonlinearity in response and interaction. A cable model consisting of two identical sagged cables in parallel connected by another lighter secondary cable is selected for investigations. Experimental results reveal that nonlinearity in the secondary cable motion induces main cables to vibrate with nonlinear motion consisting of sub-harmonic components in response in addition to simple harmonic component. Analytical investigations based on the solution of nonlinear equation of motions, derived from modal synthesis approach with substructural formulations, show early jump in the frequency response curve of main cable. Generation of closely spaced modes due to addition of secondary cable plays an important role on its controlling effects on main cable response through this type of nonlinear interaction.

Keywords

Cable system, Nonlinear interaction, Secondary cable, Passive control, Modal synthesis

INTRODUCTION

Cable system plays an important role in many of the civil engineering structures including transmission lines, guyed towers, cables-stayed bridges, suspension bridges and some space structures. Due to their lighter weight, greater flexibility and lower damping, however, cables in a structure are prone to vibrations under different types of dynamic loadings. This dynamic problem can adversely affect the human comfort and even the structural safety. Because of the importance of the cable vibration, many interesting and useful studies have been made to develop methodologies for controlling cable vibration. One of the structural means of controlling cable vibration is the application of additional secondary cables in the primary cable system and the effectiveness and applicability of this technique have been confirmed experimentally as well as analytically [1-3]. Interactions among various substructures of the primary-secondary system play an important role on control performance of the secondary cable in reducing the main cable response. Better understanding of these interactions may help greatly to design a cable structure, and the linear interaction in the primary-secondary system has been studied in the previous paper [4] in relation to the control mechanism.

Cables are, however, susceptible to large displacements under various loading condition because of its little flexural rigidity, as mentioned earlier. This larger displacement induces geometrically nonlinear behavior and this nonlinear behavior must be carefully discussed in investigations on the control mechanism of secondary cable [5].

Nonlinear vibrations of taut cables or strings were considered first by Carrier [6, 7] and whirling in strings was considered by Miles [8]. Some relatively recent works [9-12] have been devoted to the study of nonlinear vibrations of cables. Yamaguchi et al. [10] obtained nonlinear time response of horizontal and inclined cables and showed that nonlinear time responses of the cable are much dependent on the sag-to-span ratios. Al-Noury and Ali [12] considered nonlinearly coupled in-plane and out-of-plane vibrations of parabolic cables. As a result of these studies, the characteristics of nonlinear vibrations of single cables with small sag-to-span ratios have become clearer. The single cable behavior is, however, important for understanding a behavior of cable system only to some extent. Complete understanding of the system characteristics requires additional knowledge regarding the modifications encountered in the individual behavior due to interaction among different substructures, while some works have recently appeared in the literature concerning nonlinear dynamic analysis of cable system [13-15].

In the case of cable structure consisting of primary and secondary system, the nonlinearity of secondary cable interacts with the primary cable motion and the whole system motion may become nonlinear, which might be related to the controlling effect of secondary cable on main cable response. We are, therefore, motivated to investigate the effect of secondary cable in controlling the main cable response paying special attention on the nonlinear interactions among various substructures in the cable system. At first, experimental investigations have been conducted and the results are explained from the viewpoint of nonlinear theory. Analytical results are also presented on the basis of numerical analysis using a nonlinear dynamic modeling of cable. That is, the traditional substructural method with modal synthesis is adapted to derive the complete

nonlinear equations of motion for the cable system, in order to understand the nonlinear control mechanism of secondary cable.

MODEL FOR INVESTIGATION

A cable system consisting of two identical sagged cables in parallel connected by another sagged cross cable, previously studied for the control performance of the secondary cable [4], is analyzed in this paper. The schematic diagram of the model is shown in *Figure 1* and the specifications of cables are listed in *Table 1*. The connecting cross cable is designated as a secondary cable since its weight and stiffness are very small in comparison with that of the two parallel, main cables. All the three cables in the model are wire strand ropes with diameter of 1.5 mm and 0.81 mm for main and secondary cables, respectively. Several pieces of lead weights were used for both the main and secondary cables in order to adjust the model weight. It should be noted that the sag of secondary cable is set to be same as that of main cable in order to make the natural frequencies of secondary cable close to those of main cable (see Appendix A for details). This is due to an expectation of Tuned Mass Damper effect in which the response of secondary cable becomes very large caused by the internal resonance.

EXPERIMENTAL RESULTS AND NONLINEARITY IN RESPONSE

Experimental Method and Measurements

One of main cables of the cable system was excited applying harmonically varying force in the lateral direction, using electro-magnetic vibration exciter, at the point shown in Fig. 1. Steady state responses of the cables at appropriate positions, as depicted also in Fig.1, were then measured in both horizontal and vertical directions by using a video-tracker system. To assure the excitation only in the lateral direction, much attention was paid to prevent any in-plane component of excitation. The input excitation and the output response of the cable system were measured simultaneously using different cameras in order to make the measurement more accurate. The experiment was done with constant excitation amplitude and the frequency was increased with small increment at every step. Particularly near the resonant region, the frequency increment was reduced as necessary. At every step, measurement was done after some time of changing the excitation frequency in order to allow the system to reach the condition of steady state response at the new frequency. Averaged amplitude was obtained from the measured time series of displacement at the position of exciter in the main cable and is used as excitation amplitude. The excitation frequency was also computed from the same data. In the construction of frequency response curves of different cables in cable system, the maximum displacement with time, or the peak displacement in steady state, at the selected locations is used as the response parameter. In this study, we investigate the behaviors of the single main cable and the cable system for two modal frequency regions; the first anti-symmetric modal frequency region of single main cable (the 2nd out-of-plane mode) around 5.0Hz and the second symmetric out-of-plane modal frequency region (the 3rd out-of-plane mode) around 7.5Hz.

System Behavior in the Second Out-of-plane Modal Region of Single Main Cable

Both the single main cable and the cable system were excited in the out-of-plane direction with excitation amplitude of 0.11 mm. Because the excitation frequency was first restricted in the region of the second out-of-plane mode, which is anti-symmetric, the responses were measured at the quarter span positions of the main and secondary cables, depicted in Fig. 1. It is noted that the in-plane response of main cable and the out-of-plane response of secondary cable were insignificant in this case.

The frequency response curves of the out-of-plane motions for the single main cable and the excited main cable in the cable system are shown in Fig. 2(a) with the time response records at some important frequencies. It is obvious from the figure that the frequency response curve of the main cable in the system is changed into two-peaks curve, as was studied in the previous paper [4]. The time series corresponding to the peak response of the single main cable is nearly simple harmonic, while the motion of the main cable in the system corresponding to the main peak becomes multi-harmonic caused by the nonlinearity. As for the secondary cable, the frequency response curve of the in-plane motion is shown in Fig. 2(b) with the time responses corresponding to those of the main cable in Fig. 2(a). It is evident from the figure that the response of secondary cable is highly nonlinear (multi-harmonic) at the greater responses. Since the single main cable response is simple harmonic but the main cable response in the system is multi-harmonic, secondary cable nonlinearity (consisting of multi-harmonic components) might be the main controlling factor in inducing the main cable to vibrate with nonlinear motion with several harmonic components in the response.

In order to identify the nonlinear components in both main and secondary cable motions in the cable system, the measured time series were analyzed by FFT. The results in the power spectral density curves are shown in Figs. 3(a) and (b). These figures reveal the existence of half sub-harmonic component in the main and secondary cable responses. Due to the existence of the nonlinearity in the responses, the main cable response is reduced to some extent.

The existence of the fractional harmonic components in the responses can be explained on the basis of the free vibration characteristics of system. Fig. 4 shows the first fifteen normal modes along with corresponding natural frequencies of the cable system, which were obtained by the free-vibration analysis of the cable system based on the finite element method [4]. The closely spaced natural frequencies, obvious from Fig. 4, are nearly commensurable in many combinations. This commensurable relationship indicates a possibility of internal resonance, causing the corresponding modes to be strongly coupled, as well as an existence of combinational resonance for harmonic excitation of circular frequency Ω such as $\omega_1 + \omega_2 \approx \Omega$, which corresponds to the frequency of approximately 5.00 Hz in this case. The simultaneous existence of internal and combination resonance resulted in the generation of the fractional harmonics with the circular frequency of $\frac{1}{2}\Omega$, because of a cubic type of nonlinearity in the cable vibration [16].

On the basis of above discussions and experimental evidences, it can be said that nonlinearity may become significant particularly due to large response in secondary cable. The existence of this type of sub-harmonic components should be one of the underlying factors affecting the reduction of main cable response.

System Behavior in the Third Out-of-plane Modal Region of Single Main Cable

Two sets of experiments were conducted with different excitation amplitudes in this case of frequency region around 7.5 Hz. At first, smaller excitation (excitation amplitude is 0.18 mm) was applied, and the responses were measured at the mid-span positions of the main and secondary cables simply because the third out-of-plane mode is symmetric. The response of single main cable was also measured with the same excitation amplitude. Frequency response curves of the out-of-plane motion for the single cable and the excited main cable in the cable system are shown in Fig. 5(a), and the corresponding frequency response curve of the in-plane motion for the secondary cable in Fig. 5(b). It is noted that the in-plane response of main cable and the out-of-plane response of secondary cable were insignificant in this case. As can be seen from Fig. 5(a), the responses of the single cable and the excited main cable in the system are nonlinear and more or less same, while the early jump of the main cable response in the cable system is observed. As a result, response of the main cable is reduced to some extent. Another important observation is the fact that all the cable motions are nearly simple harmonic, which was confirmed by the FFT analysis. There exists, however, small amount of beating in all the responses, shown in the time series in Fig. 5, caused by the existence of two closely-spaced modes (mode-14 and mode-15 in Fig. 4) in which the two main cable motions are in-phase and out-of-phase. Because of this, constant exchange of energy from one mode to another is observed.

Secondly, the cable system and the single cable were excited with comparatively large excitation amplitude of 0.69 mm. The frequency response curves for the out-of-plane response of the main cable and the in-plane response of the secondary cable are shown in Figs. 6(a) and (b), respectively, while the coupling between the out-of-plane motion and the in-plane motion was observed in both the main and secondary cables in this case (see Appendix B for details). Significant change in the response of the main cable in the system is obvious, and the motion of the secondary cable as well as that of the main cable become multi-harmonic due to the nonlinearity, as can be seen from the time series shown in Fig. 6. However, the single main cable response remains almost simple harmonic even for the response greater than the maximum response of the main cable in the system. The FFT analysis of the time responses for the main cable and the secondary cable in the cable system shows the existence of one-third sub-harmonic component in the response, as is evident from the power spectra shown in Figs. 7(a) and (b).

The generation of this sub-harmonic component in the response can be explained in the same way as the previous section. From Fig.4, the presence of internal resonance is obvious from the commensurable relationships; $\omega_{14} \approx \omega_{15} \approx 3\omega_1 \approx 3\omega_2 \approx 3\omega_3$. In this circular frequency range corresponding to the frequency around 7.5Hz, furthermore, there exist a large number of linear relationships among the excitation circular frequency Ω and the modal circular frequencies ω, causing combinational resonance. Some examples are $\Omega \approx (\omega_7 + \omega_1) \approx (\omega_8 + \omega_1) \approx (\omega_9 + \omega_1)$ for the quadratic nonlinearity and $\Omega \approx (\omega_1 + \omega_2 + \omega_3)$, $\Omega \approx (2\omega_1 + \omega_2) \approx (\omega_1 + 2\omega_2)$ for the cubic nonlinearity. Due to the simultaneous existence of internal resonance and combinational resonance, an odd-fractional sub-harmonic component pair $\left(\frac{1}{3}\Omega, \frac{2}{3}\Omega\right)$ is observed in the responses because of the quadratic type of nonlinearity. Saturation phenomena, due to the presence of internal resonance coupled with quadratic nonlinearity, have played an important role

for existence of sub-harmonic components in the total response of the system. As a result, contributions from modes with frequencies equal to the excitation frequency have reached the upper bound and energy spills over to the lower modes. According to Dallos [17], the general form of this type of odd-fractional sub-harmonics can be obtained from the general relationship; $\omega_L = \Omega \frac{n}{2n+1}$ and $\omega_U = \Omega \frac{n+1}{2n+1}$ for n = 1, 2, 3…, where the subscripts *L* and *U* correspond to lower and upper odd-fractional sub-harmonic components, respectively. Some other researchers also observed this type of fractional harmonic pairs in many physical systems [18, 19].

Effect of Secondary Cable Nonlinearity on the Control Performance

It is obvious from the previous discussions that the source of nonlinearity from the viewpoint of multi-harmonic response in the cable system is the multi-harmonic motion of secondary cable due to its large response. This affected the motion of the main cable in several respects. For example, one additional peak around 7.34 Hz, which is caused mainly by the one-third sub-harmonic response, is observed in the frequency response curve of the main cable of the system for larger excitation amplitude in Fig. 6(a), while it is nonexistence for the smaller excitation amplitude in Fig. 5(a).

As mentioned earlier, adding secondary cable generates many closely spaced modes of the cable system, in which the magnitude of secondary cable response becomes greater for out-of-phase motions of the two main cables and smaller for in-phase motions. Some particular modes among them can be excited depending on the excitation frequency, and characterize the nonlinear response of the cable system. At the excitation frequency of around 7.34 Hz in Fig. 6, the two main cables vibrate in the main harmonics with in-phase motions and more largely in the one-third sub-harmonics with out-of-phase motions, as shown in Figs. 7(a) and 8(a), resulting very large secondary cable response only in the one-third sub-harmonics in Fig. 7(b). The main harmonics might be in the system mode-15 in Fig. 4, while the sub-harmonics is most probably due to the participation of the system mode-3 in Fig. 4, which corresponds to the first out-of-plane mode of the single main cable. This is because, when the response becomes greater, there is a tendency for the energy to flow from the higher to the lower modes in the case of existence of internal resonance [16].

At around the frequency of 7.70 Hz in Fig. 6, on the contrary, very large responses of the two main cables are dominated by the main harmonics with in-phase motions in the system mode-15, as shown in Figs. 7(a) and 8(b), and the corresponding response of the secondary cable is much smaller than the main cable (Figs. 7(a) and (b)). However, there exists enough amount of the main harmonics in the secondary cable response to have significant sub-harmonic response in the secondary cable, resulting the sub-harmonics in the main cable response with out-of-phase motions in some amount. In this way, the main cable response becomes nonlinear, containing the sub-harmonic component, due to the large response of the secondary cable with complicated nonlinear motions. As a result, the main cable response contains the contributions not only from the main harmonics in the system mode-15 but also from the one-third sub-harmonic component. This is also because of the presence of the system mode-3, corresponding to the first out-of-plane mode of the single main cable, due to energy flow from higher modes to lower modes in the presence of internal resonance.

The nonlinearity of the secondary cable, therefore, induces the main cable to vibrate in nonlinear multi-harmonic motion and thereby helps in the distribution of energy among various harmonics and among different modes. This energy distribution due to secondary cable nonlinearity is one of the important factors underlying the controlled response of the main cable.

ANALYTICAL INVESTIGATION - A COMPLETE NONLINEAR APPROACH

Derivation of Equation of Motion

An approach of substructural formulation with modal synthesis [20-22] is applied to solve the dynamic interaction problem of cable system. This is because it is convenient to explain the effect of one component, or substructure, on the other on the basis of substructural response solution. Since cables are geometrically nonlinear in nature, some modifications have been incorporated in the substructural formulation in this study [23].

For the *r-th* substructure, the dynamic position vector, $\{X\}_r$, can be decomposed into the static position vector, $\{X^0\}_r$, and the dynamic displacement vector, $\{u\}_r$, as follows.

$$\{X(s)\}_r = \{X^0(s)\}_r + \{u(s)\}_r \tag{1}$$

where s is a material coordinate designating the arc length of substructural cable.

According to the modal synthesis approach, the dynamic displacement vector is represented in the modal space as

$$\{u(s)\}_r = \left[\overline{\Phi}_{constraint}(s) \quad \overline{\Phi}_{normal}(s)\right]_r \{p\}_r \tag{2}$$

where sub-matrices $\left[\overline{\Phi}_{constraint}\right]$ and $\left[\overline{\Phi}_{normal}\right]$ are substructural constraint mode matrix and truncated normal mode matrix, respectively. $\{p\}_r$ in Eq. (2) is the generalized coordinate vector for the *r-th* substructure. In the case of traditional substructural formulation, system matrices corresponding to the substructural generalized coordinates are first derived from direct assembly of the substructural matrices. A linear transformation matrix is then obtained by considering kinematic compatibility conditions at the junctions of substructures. Finally, performing the linear transformation, the system matrices corresponding to the independent generalized coordinates are obtained.

In the case of nonlinear system, however, this type of linear transformation is not possible. In order to overcome this difficulty in the formulation, the substructural displacement in Eq. (2) is expressed in terms of independent generalized coordinates of the system for all the substructures, considering displacement compatibility at inter-substructural junctions. Let us consider n_1, n_2 and n_s are the number of substructural modes for the 1st main cable, the 2nd main cable and the secondary cable, respectively. Assuming the substructural generalized coordinates for each main cable as independent from generalized coordinates of other main cable and the secondary cable, we can express Eq. (2) for two main cables as

$$\{u(s)\}_{m1} = \left[\Phi(s)\right]_{m1} \{q\}_{m1} \tag{3.a}$$

$$\{u(s)\}_{m2} = \left[\Phi(s)\right]_{m2} \{q\}_{m2} \tag{3.b}$$

where $\{q\}_{m1}$ and $\{q\}_{m2}$ are the independent generalized coordinates for the 1st and 2nd main cables and $[\Phi(s)]_{m1}$ and $[\Phi(s)]_{m2}$ are the substructural mode shape matrices for

these two main cables, respectively. If the total substructural degrees of freedom are k_1 and k_2 for the 1st and 2nd main cables, $[\Phi(s)]_{m1}$ and $[\Phi(s)]_{m2}$ are (k_1 x n_1) and (k_2 x n_2) square matrices, respectively.

As for the substructural displacement vector for the secondary cable, we can expand it into three components, corresponding to constraint modes and normal modes, as follows.

$$\{u(s)\}_s = [\Phi(s)]_{sc1}\{q\}_{sc1} + [\Phi(s)]_{sc2}\{q\}_{sc2} + [\Phi(s)]_{sn}\{q\}_{sn} \tag{4}$$

$\{q\}_{sc1}$ and $\{q\}_{sc2}$ in Eq. (4) are generalized coordinate vectors for constraint modes corresponding to the junctions of seconadry cable to the 1st main cable and to the 2nd main cable, respectively, which are completely dependent on the generalized coordinate vectors of the 1st and 2nd main cable. It is noted that the order of $\{q\}_{sc1}$ and $\{q\}_{sc2}$ is equal to the number of degrees of freedom at the respective junction node (for this study 3; x, y and z displacements). $\{q\}_{sn}$ in Eq. (4), on the contrary, corresponds to the substructural normal modes of secondary cable and independent of any other generalized coordinates.

According to the definition of constraint modes, at any instance of time, $\{q\}_{sc1}$ and $\{q\}_{sc2}$ can be the displacement vectors at the junction nodes j_1 and j_2. That is,

$$\{q\}_{sc1} = \{u\}_{j1} = [\Phi]_{m1}^{j1}\{q\}_{m1} \tag{5.a}$$

$$\{q\}_{sc2} = \{u\}_{j2} = [\Phi]_{m2}^{j2}\{q\}_{m2} \tag{5.b}$$

Substituting Eqs. (5.a, b) into Eq. (4) leads to

$$\{u(s)\}_s = [\Phi(s)]_{sc1}[\Phi(s)]_{m1}^{j1}\{q\}_{m1} + [\Phi(s)]_{sc2}[\Phi(s)]_{m2}^{j2}\{q\}_{m2} + [\Phi(s)]_{sn}\{q\}_{sn} \tag{6}$$

After matrix multiplications and adding the sub-matrices in Eq. (6), we can express the above equation in terms of independent generalized coordinates as

$$\{u(s)\}_s = [\overline{\Phi}(s)]_s \begin{Bmatrix} \{q\}_{m1} \\ \{q\}_{m2} \\ \{q\}_{ns} \end{Bmatrix} \tag{7}$$

The mode shape matrix, $[\overline{\Phi}(s)]_s$, in the above equation is the final form of modified mode shape matrix for the secondary cable.

Static configuration of the cable system, $\{X^0\}$, is determined by nonlinear finite element analysis method [24] using 3-node elements with shape function matrix, $[N(s)]$. Since the dynamic displacement vector for the cable element can be also represented in terms of the shape function, the dynamic position vector in the cable element is given as

$$\{X(s)\}_e = [N(s)]\{X_n^0\} + [N(s)][\Phi_n]\{q\} \tag{8}$$

where the subscripts e and n represent quantities evaluated in the element and at the nodal points, respectively.

Lagrangian strain, ε_s, is evaluated for the cable element by using the nonlinear strain-displacement relation. That is,

$$(\varepsilon_s)_e = \{X_n^0\}^T[N']^T[N'][\Phi_n]\{q\} + \frac{1}{2}\{q\}^T[\Phi_n]^T[N']^T[N'][\Phi_n]\{q\} \tag{9}$$

where $(')$ indicates differentiation with respect to the arc length, s. The second term of Eq. (9) is the nonlinear part of the Lagrangian strain, ε_s^{nl}.

The equation of motion for the system's generalized coordinate can be derived by applying the principle of virtual work:

$$\sum_e \int_0^L \{\delta u\}_e^T \{f\}_e ds + \{\delta u_n\}^T \{r\} - \sum_e \int_0^L \left(A\sigma_s \delta\varepsilon_s\right)_e ds - \sum_e \int_0^L \left(A\sigma_0 \delta\varepsilon_s^{nl}\right)_e ds = 0 \qquad (10)$$

where $\{f\}$, $\{r\}$, A and L are the distributed load vector, the nodal load vector, the cross-sectional area and the element length, respectively. σ_0 is the static stress with self-weight, while σ_s is Kirchhoff's stress. It should be noted that the static stress does work only on the nonlinear component of the dynamic strain [25]. Substituting Eqs. (8) and (9) into Eq. (10) with some manipulations leads to the final expression of the equation of motion.

$$[M]\{\ddot{q}\} + [C]\{\dot{q}\} + [K]\{q\} + \{g(q)\} - \{r_q\} = 0 \qquad (11)$$

In this equation of motion, the mass matrix, $[M]$, the linear stiffness matrix, $[K]$, the geometrically nonlinear stiffness term, $\{g(q)\}$, and the generalized force vector ,$\{r_q\}$, are represented as follows.

$$[M] = \sum_e m \int_0^L [B_1] ds \qquad (12.a)$$

$$[K] = \sum_e \left[(\sigma_0 A)_e \int_0^L [B_2] ds + (EA)_e \int_0^L \{b\}\{b\}^T ds \right] \qquad (12.b)$$

$$\{g(q)\} = \frac{1}{2}\sum_e (EA)_e \int_0^L \left(\{q\}^T [B_2]\{q\}\right)[B_2]\{q\} ds + \sum_e (EA)_e \int_0^L \left(\{b\}^T \{q\}\right)[B_2]\{q\} ds + \frac{1}{2}\sum_e (EA)_e \int_0^L \left(\{q\}^T [B_2]\{q\}\right)\{b\} ds \qquad (12.c)$$

$$\{r_q\} = [\Phi]^T \{r\} \qquad (12.d)$$

where m is the cable mass per unit length and

$$[B_1] = [\Phi_n]^T [N]^T [N][\Phi_n], \quad [B_2] = [\Phi_n]^T [N']^T [N'][\Phi_n] \qquad (13a, b)$$

$$\{b\} = \{X_n^0\}^T [N']^T [N'][\Phi_n] \qquad (13.c)$$

Solution Methodology

Six substructural normal modes and necessary constraint modes for main and secondary cables [4], shown in Fig. 9, are considered for the substructural formulation to compute each term in Eq. (11). As for the evaluation of damping matrix $[C]$, the energy-based damping theory is used on the basis of experimentally obtained damping properties of cables [14].

In order to discuss analytically the nonlinear and interactive responses of the cable system in the frequency range corresponding to the third out-of-plane modal region of single main cable, the solution for the *i-th* generalized coordinate in the equations of motion in Eq. (11) is assumed in terms of Fourier series as follows, and the harmonic balance method [26, 27] is applied to determine the Fourier amplitudes and the corresponding phase angles.

$$q_i = A_0^i + A_1^i \cos\left(\frac{1}{3}\Omega t + \theta_1^i\right) + A_2^i \cos\left(\frac{2}{3}\Omega t + \theta_2^i\right) + A_3^i \cos\left(\Omega t + \theta_3^i\right) \qquad (14)$$

where A_0^i is the constant component of the *i-th* generalized coordinate; A_1^i, A_2^i, *and* A_3^i are the amplitudes of one-third sub-harmonic component, two-third sub-harmonic component and the simple harmonic component *of the i-th* generalized coordinate,

respectively; $\theta_1^i, \theta_2^i, \theta_3^i$ are the corresponding phase angles; Ω is the excitation circular-frequency.

Nonlinearity in Response and Early Jump in Frequency-Response Curves

One of the main cables is excited by applying harmonically varying concentrated load ($Force=P \cos \Omega t$) in the out-of-plane direction of main cable at a distance of 0.75 % of span length from the support. Fig. 10 shows computed frequency response curves for the single cable and for the main cable in the cable system under the condition of P = 5.0 N, which was selected for simulating the maximum peak-displacement comparable to that measured in the experiment. Both the curves were obtained from the nonlinear analysis considering all nonlinear terms in Eq. (7). The controlling effect of secondary cable in reducing the main cable response is obvious from Fig. 10. That is, the early jump in the frequency response curve of main cable in the cable system is one of the most important factors in controlling the response.

This can be explained on the basis of the existence of many closely spaced modes in the cable system. The previous investigation [4] shows that there exist two modes at the frequencies of 7.55 Hz and 7.57 Hz corresponding to the system mode-14 and the system mode-15 in Fig. 4. Two main cable motions are out-of-phase in the system mode-14, while they exhibit in-phase motion in the system mode-15. Because of out-of-phase motions of two main cables in the system mode-14, the secondary cable motion is dominant and thereby the main cable motion becomes limited. On the other hand, in-phase motion in the system mode-15 causes the secondary cable to vibrate with asymmetric modal contribution with dominant motion in the main cables. From this observation, it can be understood that the symmetric motion of the secondary cable makes the main cable in the system stiffer than the case when the secondary cable motion is asymmetric, in the sense that the symmetric motion of the secondary cable constrains the main cables' motion significantly.

In the case of nonlinear analysis, above mentioned modes are also existent but the system can vibrate with these linear modes up to frequency considerably larger than the corresponding natural frequencies. This is evident from the frequency response curve of the single cable in Fig. 10. For the frequency range considered in this figure, the single cable response is a contribution only from the 5th mode or the 3rd out-of-plane mode. The natural frequency of this normal mode is 7.43 Hz, but the peak response with this modal vibration occurs at the frequency of around 12.0 Hz due to the consideration of nonlinearity, which is evidenced also in the experimental investigation of single cable as shown in Fig. 6(a). In the case of the cable system, there exist two dominant modes at the frequency of 7.55 and 7.56 Hz with main contribution from the 3rd out-of-plane mode. After the first smaller peak at frequency 7.28 Hz in Fig. 10, the cable system begins to vibrate with the 15th normal mode in which two main cables are in in-phase motion. The existence of this motion prevails up to the frequency of 8.94 Hz, which is obvious from the vibration mode shown in Fig. 10 for 8.93 Hz. However, there exists another mode with out-of-phase motion of two main cables and symmetric motion of the secondary cable, that is, the system mode-14. Nonlinearity plays a role in such a way that the contribution of system mode-14 becomes existent beyond 8.94 Hz. Since the main cable in the system mode-14 is stiffer than that in the system mode-15, as previously discussed, the response of the main cable in the system suddenly becomes smaller and early jump phenomenon is observed because of the existence of the system

mode-14. This early jump in the frequency response curve is one of the important factors affecting the control performance of the secondary cable.

Nonlinear Interaction and Energy Redistribution Among Substructural Modes

The addition of secondary cable has another effect of causing the excitation energy to be distributed among the different substructural modes due to nonlinear interaction. In the case of single cable, the response in the resonance region is dominated mainly by the normal mode corresponding to the frequency. Due to the addition of secondary cable, on the contrary, several substructural modes have considerable contribution in the response in the system.

This is obvious from the variation of generalized coordinates with excitation frequency as shown in Fig. 11 for the excited main cable and Fig. 12 for the secondary cable. Only the constant component (A_0) and the amplitude of simple harmonic component (A_3) for different generalized coordinates are shown in the figures, because the contributions from the sub-harmonic components were found very small under the loading conditions considered in the analysis. It is noted that the existence of sub-harmonic component can be observed only under certain loading conditions with a particular set of initial values of the generalized, which is discussed in the next section.

It is obvious in Fig. 11(a) that the contributions from the first out-of-plane normal mode (the third mode in Fig. 9(a)) and the second out-of-plane normal mode (the fifth mode in Fig. 9(a)) are relatively large, while the third out-of-plane normal mode is dominant due to the resonance. Furthermore, not only the out-of-plane modes but also the in-plane substructural modes are excited with considerable contribution in the system responseas shown in Fig. 11(b). Strong coupling between the out-of-plane motion and the in-plane motion of main cables are observed near the smaller response peaks at 6.5 Hz and 7.1 Hz.

In the main resonant region around 8 Hz, the contribution of generalized coordinates for the lower out-of-plane modes of the main cable in Fig. 11(a), can be explained in relation to the response of the secondary cable in Fig. 12(a). Only constraint modes are excited for the secondary cable (Fig 12(a)), while normal mode contributions in the total response of secondary cable are very small (Fig. 12(b)). Actually, secondary cable acted as a medium of continuity between two main cables and thereby causing coupling between the motions of the two main cables. As mentioned previously, the secondary cable connects two main cables at a distance of 5/12 of the main cable span from the left supports, which is at halfway of two node points of the second and third out-of-plane normal modes. During the vibration of the cable system, the effects of the secondary cable can be considered as the main cable vibration with additional dynamic load at this junction point. This dynamic force causes the lower out-of-plane modes to be excited due the secondary cable response. As a result, total excitation energy is distributed among different substructural modes. This energy redistribution among different substructural modes is one of the underlying factors related to the control mechanism of the secondary cable.

Excitation Amplitude and Modal Jump

Depending on the excitation force amplitude, the composition of the response becomes significantly different. For smaller excitation force amplitude, the response is almost similar to the linear response. But as the response increases with increasing excitation force, the response contains considerable contribution from several lower modes of each

substructure. Figs. 13 and 14 represent the variation of generalized coordinates corresponding to different substructural modes with excitation force amplitude, P, for the excited main cable and the secondary cable, respectively. The excitation frequency is 7.6 Hz which is very near to the natural frequency of system mode-14 (f=7.551 Hz) and system mode-15 (f=7.566 Hz). As can be seen in these figures, multi-valued response is possible for each substructure depending on the excitation force amplitude. As discussed previously, constraint modes are excited significantly for the secondary cable (Fig 14(a)), while contributions from most of the normal modes are small (Fig. 14(b)). However, contribution from 6^{th} normal mode (10^{th} substructural mode) has become bigger.

As shown in Fig. 13(a) for the excited main cable, A_3 of the generalized coordinate corresponding to the 7th substructural mode increases sharply for smaller excitation and it reaches a maximum value at around 2.66 N of excitation force amplitude. For excitation amplitude greater than this, three distinct magnitudes are possible for each generalized coordinates for a given excitation. In addition to this, coupling between in-plane and out-of-plane normal modes has become obvious from Fig. 13(b), and contribution from 4^{th} normal mode (6^{th} substructural mode) is bigger in the main cable response. This coupling should be due to the presence of secondary cable in the system, what makes the motions of two main cables inter-dependent on each other.

One of the three values is possible in reality depending on the sequence of excitation. If excitation increases from zero, the generalized coordinate corresponding to the 7th substructural mode will increase and reach the maximum value at the excitation of 2.66 N. After that, this generalized coordinate reduces in magnitude while the generalized coordinates corresponding to the 3rd and 5th substructural modes (the 1st and 3rd normal modes) increase up to the excitation of around 6.7 N. At this stage, the contributions of the 3rd and 5th substructural modes become greater than that of the 7th substructural mode. Further increase in the excitation causes the system to be unstable and jump occurs from the point *b* to *c* and the generalized coordinate corresponding to the 7th mode again become greater than that of the 3rd and 5th mode. Beyond this excitation, the generalized coordinates increase with smaller rate and follow the path from the point *c* to *d*. On the other hand, in the case of decreasing the excitation, different path will be followed. All the generalized coordinates reduce with smaller rate from the point indicated by *d* to the point *f* without exhibiting any jump at the point *c*. But after the point *f*, further decrease in the excitation results in jump from the higher values to lower values of generalized coordinates. The path between the points *b* and *f* is unstable and can never be traversed.

The jump phenomena observed here is, actually, related to the existence of different vibration modes with closely spaced frequencies, due to the existence of secondary cable in the system. The system vibrates with the system mode-15 and it becomes saturated at the excitation amplitude of 2.66 N. Further increase in the excitation energy causes the energy transfer from this mode to the system mode-14. This energy-sharing situation can exist up to the point *b*, beyond which the vibration energy cannot be accommodated with the combination of modes. Therefore, the system jumps from the in-phase motion of main cables to the complete out-of-phase motion to accommodate the increased excitation energy. The diagram in Fig. 15, showing the vibration mode at different excitation amplitudes, reveals this change of vibration modes depending on the excitation. It is obvious from Fig. 15(c) that the response at the mid-span of main cable is controlled, but that the response at around quarter span becomes greater. Due to this

vibration localization, apparently, negative controlling effect can exist, while it can be predicted from this phenomenon that nearly even vibration in the whole span might be possible by connecting secondary cable at appropriate location having some appropriate properties. Positive controlling effect can be expected under this type of nearly even vibration along span length.

CONCLUDING REMARKS

Investigations, based on both experimental and numerical nonlinear analysis, revealed some important phenomena providing useful information regarding the controlling effect of secondary cable and the underlying mechanism, as summarized as follows.

1) Due to the addition of secondary cable, different substructural cables can interact because of the secondary cable nonlinearity. One of the important effects of this nonlinear interaction is the early jump in the frequency response curve, whereby the maximum response of main cable is reduced significantly. This type of early jump, observed in the experimental as well as numerical investigations, plays an important role in reducing the maximum response of main cable in the cable system. The transition of vibration modes due to nonlinear interaction is the underlying factor for this phenomenon to be occurred.

2) Secondary cable nonlinearity can induce the whole system to vibrate with multi-harmonic and multi-modal response. In this way, the total excitation energy can be redistributed among the different substructural modes. This type of energy transfer from higher modes to lower modes plays an important role in the reduction of the main cable motion.

3) Depending on the level of excitation, the vibration pattern of the system may change significantly and multi-valued response is found in this study. Another important observation is the jumping from one mode to another depending on the excitation force. This jumping may cause vibration localization whereby negative controlling effect can be observed at some location. But, it might be possible to minimize this vibration localization using appropriate arrangement of the secondary cable, whereby positive controlling effect of secondary cable can be expected.

Appendix A. Natural frequencies of single cable

The n-th natural frequency, f_n, of a single cable with the length, L, the mass per unit length, m, and the horizontal component of cable tension, H, is represented by Eq. (A1) if the frequency is far from the modal crossover point [28].

$$f_n = \frac{n}{2L}\sqrt{\frac{H}{m}} \tag{A1}$$

It should be noted that this formula gives the exact value of the n-th natural frequency in the cases of the in-plane motion with the antisymmetric mode and the out-of-plane motion, while it becomes erroneous in the frequency region of modal crossover in the case of the symmetric in-plane mode.

The horizontal component of cable tension can be evaluated from the initial configuration of cable, which is characterized by the sag of the cable, f. In the case of a shallow cable with small sag, its initial configuration becomes a parabola and the horizontal cable tension can be derived as

$$H = \frac{mgL^2}{8f} \tag{A2}$$

where g is the gravitational acceleration [28].

Substituting Eq. (A2) into Eq. (A1) leads to

$$f_n = \frac{n}{4\sqrt{2}}\sqrt{\frac{g}{f}} \tag{A3}$$

where the n-th natural frequency is now represented in terms of the sag of the cable. Therefore, the natural frequencies of the secondary cable can be close enough to those of the main cable by setting the secondary cable's sag to be same as the main cable's one.

Appendix B. Coupling between in-plane and out-of-plane responses in the cable system

One interesting phenomenon in nonlinear cable dynamics is the coupling of the in-plane and out-of-plane motions. Under the harmonic planar excitation, the planar response becomes unstable and a non-planar whirling motion occurs when the response amplitude exceeds a critical level. Even in this experimental investigation where one of the main cables was excited in the out-of-plane direction, couplings between the out-of-plane and in-plane responses were measured for both the main and secondary cables in the case of the third out-of-plane modal excitation with the large excitation amplitude of 0.69mm.

Figure B1 shows the paths of the mid span motions in the vertical planes for (1) the excited main cable, (2) the secondary cable and (3) the non-excited main cable for different excitation frequencies. The existence of the coupling is obvious from the figure, and the coupling characteristics, represented by the motion path, is significantly different depending on the excitation frequency. However, it should be noted that the out-of-plane and in-plane motions dominate all the responses of the main and secondary cables in Fig.B1, respectively. Because of this, the nonlinear behaviors of the out-of-plane response in the main cable and the in-plane response in the secondary cable are only discussed in this paper.

References

1 Hojo, T., Yamazaki, S., Yamaguchi, H. Experimental study on countermeasure for man-induced vibrations of suspension structure. Proc. Int. Symp. Cable Dynamics, Liege. Liege: A.I.M., 1995: 461-468.

2 Yamaguchi, H. Control of cable vibrations with secondary cables. Proc. Int. Symp. Cable Dynamics, Liege. Liege: A.I.M., 1995: 445-452.

3 Alauddin, Md., Yamaguchi, H. Control of cable vibration through interaction among main and secondary cables. Proc. the 2nd World Conference on Structural Control, Kyoto, vol.2, Wiley, 1999: 1303-1312.

4 Yamaguchi, H., Alauddin, Md., Poovarodom, N. Dynamic characteristics and vibration control of a cable system with substructural interactions, Engineering Structures 2001; 23: 1348-1358.

5 Alauddin, Md., Yamaguchi, H. Nonlinear effects of secondary cable on its control performance. Proc. the 3rd Int. Conf. Motion and Vibration Control, vol.2, 1996: 36-41.

6 Carrier, G.F. On the nonlinear vibration problem of the elastic string, Quaterly J. Applied Mathematics 1945; 3: 157-165.
7 Carrier, G.F. A Note on the vibrating string, Quaterly J. Applied Mathematics 1949; 7: 97-101.
8 Miles, J.W. Stability of forced oscillation of a vibrating string, J. Acoustical Society of America 1965; 38: 855-861.
9 Hagedorn, P. and Schaffer, B. On nonlinear free vibrations of an elastic cable, Int. J. Nonlinear Mechanics 1980; 15: 333-340.
10 Yamaguchi, H., Miyata, T. and Ito, M. Time response analysis of a cable under harmonic excitations, Proc. Japan Society of Civil Engineers 1981; 308: 37-45 (in Japanese).
11 Luongo, A., Rega, G. and Vestroni, F. Mono-frequent oscillations of a nonlinear model of a suspended cable, J. Sound and Vibration 1982; 82 (1): 247-259.
12 Al-Noury, S.I. and Ali, S.A. Large amplitude vibrations of parabolic cables, J. Sound and Vibration 1985; 101: 451-462.
13 Yamaguchi, H. and Jayawardena, L. Analytical estimation of structural damping in cable structures, J. Wind Eng. Ind. Aerodyn. 1992; 41-44: 1961-1972.
14 Yamaguchi, H. and Nagahawatta, H. D. Damping effects of cable cross ties in cable- stayed bridges, J. Wind Eng. Ind. Aerodyn. 1995; 54/55: 35-43.
15 Morris N.F. The use of modal superposition in nonlinear dynamics, J. Computers and Structures 1977; 7: 65-72.
16 Nayfeh, A.H., and Mook, D.T. Nonlinear oscillations. New York: Wiley, 1979.
17 Dallos, P.J. On the generation of odd-fractional subharmonics, J. Acoustical Society of America 1966; 40: 1381-1391.
18 Adler, L. and Breazeale, M.A. Generation of fractional harmonics in a resonant ultrasonic wave system, J. Acoustical Society of America 1970; 48: 1077-1083.
19 Eller, A.I. Fractional-harmonic frequency pairs in nonlinear systems, J. Acoustical Society of America 1973; 53: 758-765.
20 Hurty, W.C. Dynamic analysis of structural systems using component modes, AIAA Journal 1965; 3 (4): 678-685.
21 Craig, R.R.Jr. and Bampton, M.C.C. Coupling of substructures for dynamic analysis, AIAA Journal1968; 6 (7): 1313-1319.
22 Benefield, W.A., and Hruda, R.F. Vibration analysis of structures by component mode substitution, AIAA Journal 1971; 9 (7): 1255-1261.
23 Alauddin, Md. Vibration control and its mechanism in cable system with secondary cable. Doctoral dissertation, Saitama University, Japan, 1998.
24 Henghold, W.M. and Russel, J.J. Equilibrium and natural frequencies of cable structures (A nonlinear finite element approach), J. Computers and Structures 1976; 6: 267-271.
25 Washizu, K. Variational methods in elasticity and plasticity. Pergamon Press, 3rd ed., 1982.
26 Timoshenko, S.P., Young, D.H. and Weaver, Jr.W. Vibration Problems in Engineering. New York: Wiley, 4th ed., 1974.
27 Ueda, T. Nonlinear free vibrations of conical shells, J. Sound and Vibration 1979; 64 (1): 85-95.
28 Irvine M. Cable structures, MIT Press, 1981.

Captions of Tables and Figures

Table 1 Specification of main and secondary cables

Figure 1 Schematic diagram of the model of cable system

Figure 2 Frequency response curves for (a) main cable and (b) secondary cable in the second modal frequency range (excitation amplitude = 0.11 mm)

Figure 3 Power spectral density curves for (a) main cable and (b) secondary cable in the system in the second modal frequency range (excitation amplitude = 0.11 mm)

Figure 4 System normal modes with natural frequencies

Figure 5 Frequency response curves for (a) main cable and (b) secondary cable in the third modal frequency range (excitation amplitude = 0.18 mm)

Figure 6 Frequency response curves for (a) main cable and (b) secondary cable in the third modal frequency range (excitation amplitude = 0.69 mm)

Figure 7 Power spectral density curves for (a) main cable and (b) secondary cable in the system in the third modal frequency range (excitation amplitude = 0.69 mm)

Figure 8 Time responses at selected frequencies of Fig. 6(a) for both of two main cables showing their phase relationship (excitation amplitude = 0.69 mm)

Figure 9 Substructural modes for main and secondary cables

Figure 10 Computed frequency response curves for single main cable and main cable in the system with vibration modes at maximum response and after jump

Figure 11 Computed responses of generalized coordinates with excitation frequency for excited main cable. (a) out-of-plane modes; (b) in-plane modes ($P=5.0$ *N*)

Figure 12 Computed responses of generalized coordinates with excitation frequency for secondary cable. (a) constraint modes; (b) normal modes ($P=5.0$ *N*)

Figure 13 Computed responses of generalized coordinates with excitation force amplitude for excited main cable. (a) out-of-plane modes; (b) in-plane modes ($f=7.6$ *Hz*)

Figure 14 Computed responses of generalized coordinates with excitation force amplitude for secondary cable. (a) constraint modes and (b) for normal modes ($f=7.6$ *Hz*)

Figure 15 Vibration modes with different excitation force amplitudes ($f=7.6$ *Hz*)

Figure B1 Path of mid span motion in vertical plane for (1) excited main cable, (2) secondary cable and (3) non-excited main cable at different excitation frequencies: (a) 6.95Hz, (b) 7.34Hz, and (c) 7.71Hz with the excitation amplitude of 0.69mm.

Table 1. Specifications of main and secondary cables

Cables	Total mass (g)	Weight		Span (m)	Sag (m)	Sag ratio (%)	Horizontal tension (N)	EA (kN)
		Mass (g)	Spacing (m)					
Main cable	547.0	15.0	0.090	3.10	0.050	1.6	41.5	353
Secondary cable	11.5	0.9	0.047	0.60	0.050	8.3	0.169	103

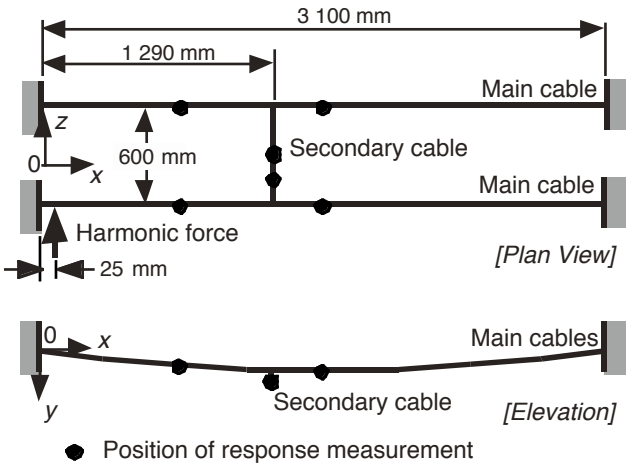

Engineering Structures
Yamaguchi, H. and Alauddin, Md.
Figure 1

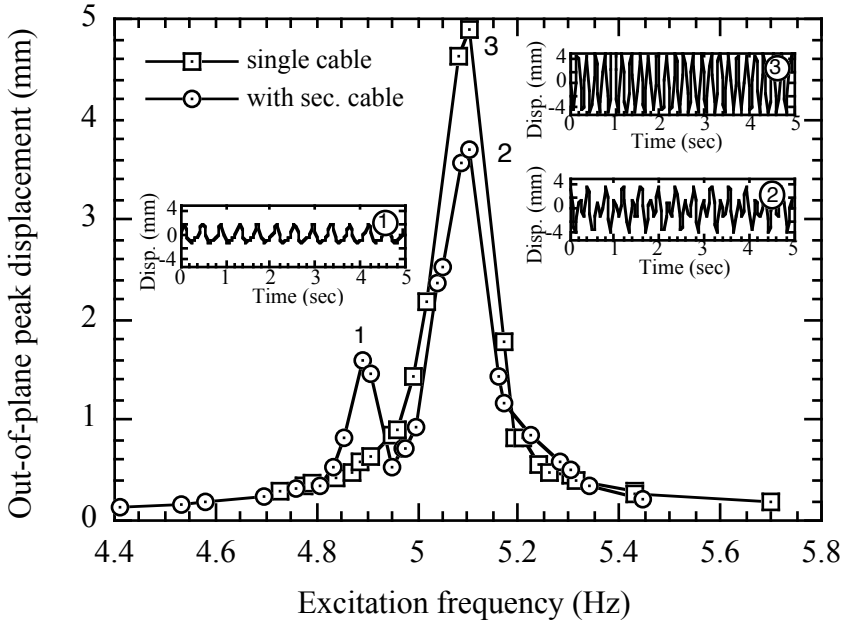

(a) Frequency response curves for main cables

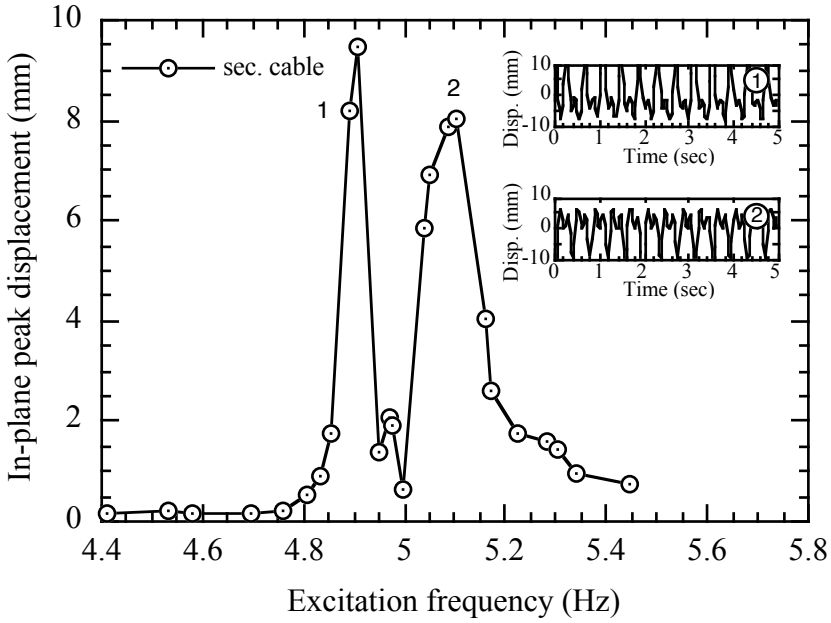

(b) Frequency response curve for secondary cable

Engineering Structures
Yamaguchi, H. and Alauddin, Md.
Figure 2

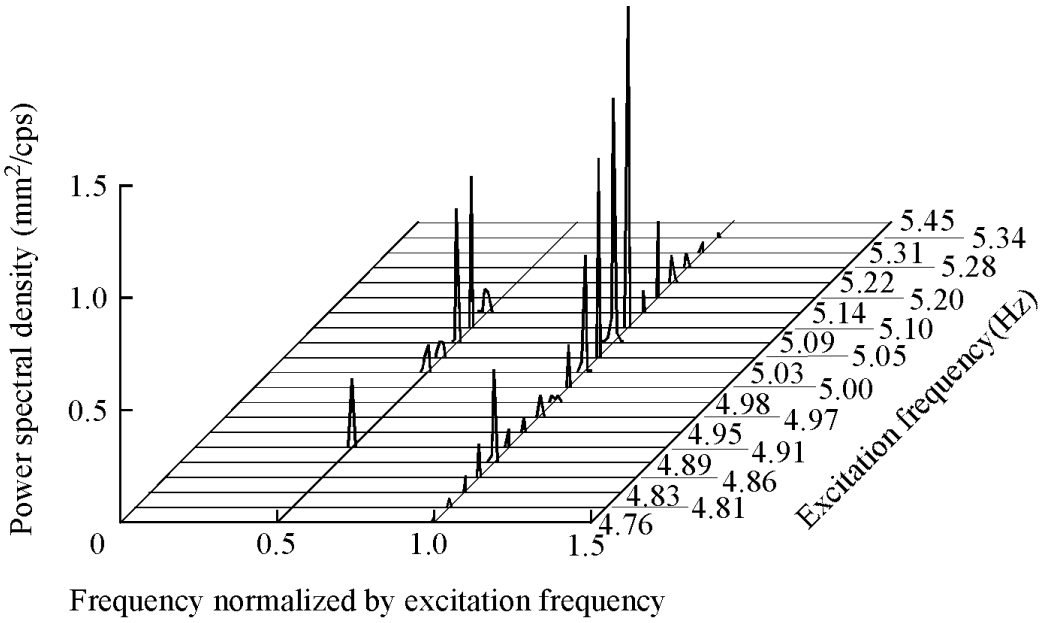

(a) Power spectral density for main cable

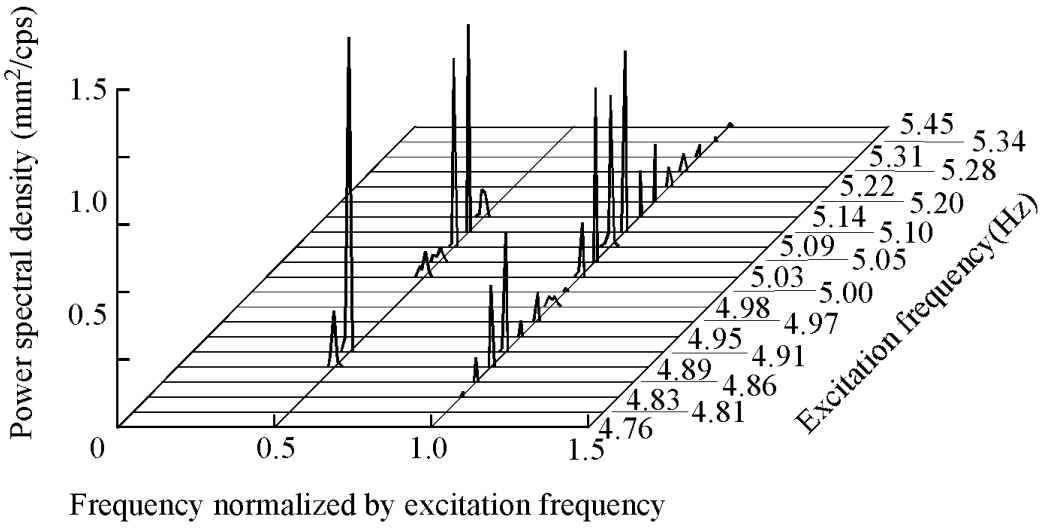

(b) Power spectral density for secondary cable

Engineering Structures
Yamaguchi, H. and Alauddin, Md.
Figure 3

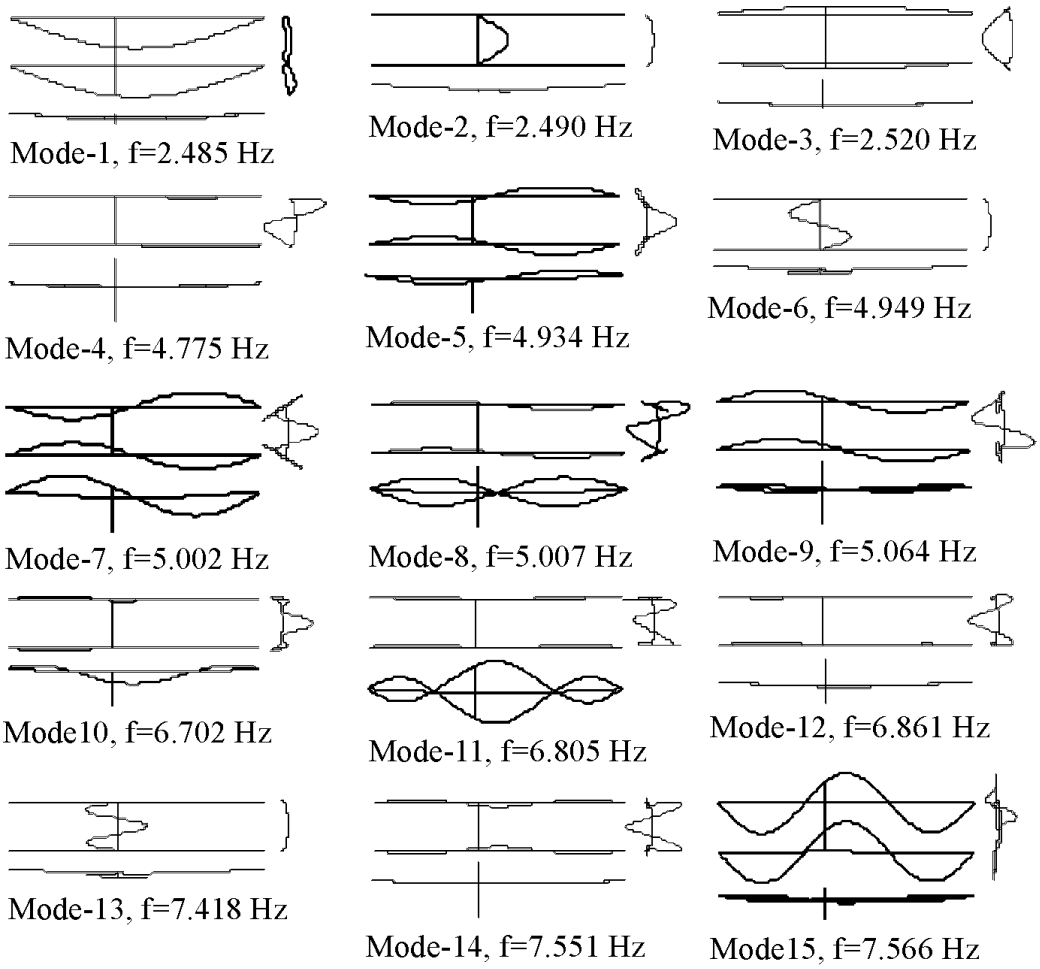

Engineering Structures
Yamaguchi, H. and Alauddin, Md.
Figure 4

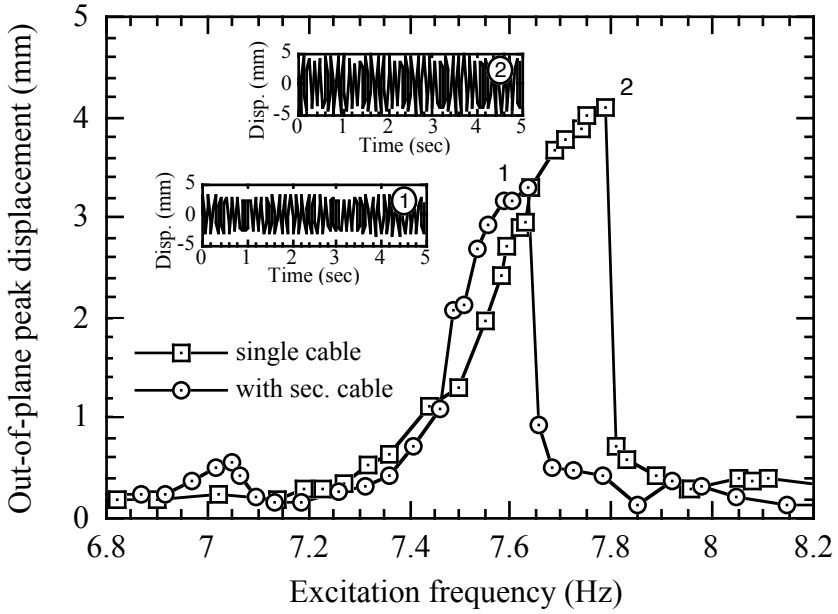

(a) Frequency response curves for main cables

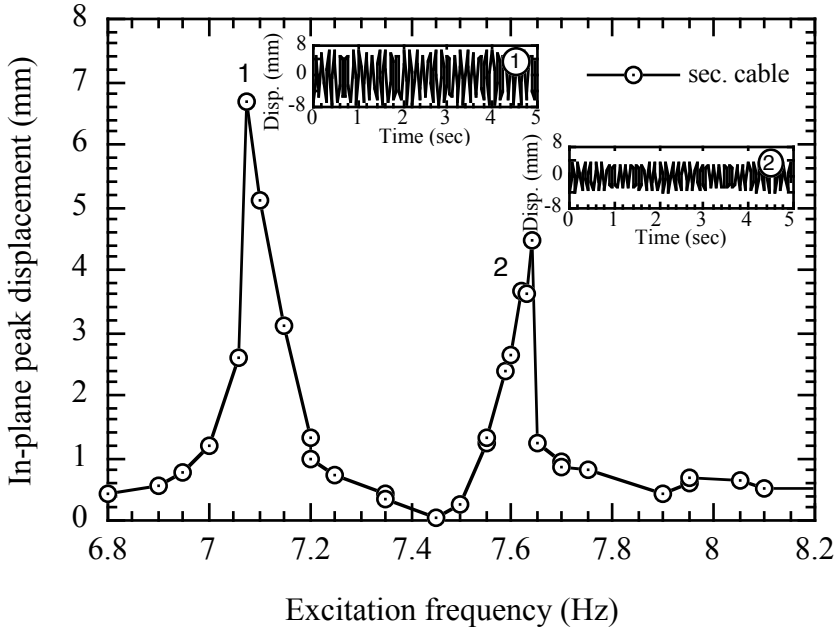

(b) Frequency response curve for secondary cable

Engineering Structures
Yamaguchi, H. and Alauddin, Md.
Figure 5

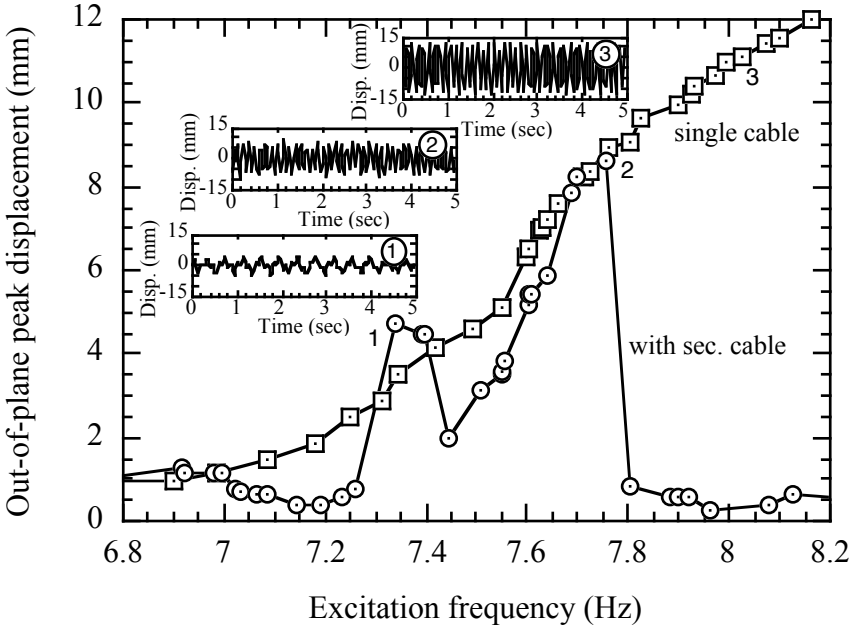

(a) Frequency response curves for main cables

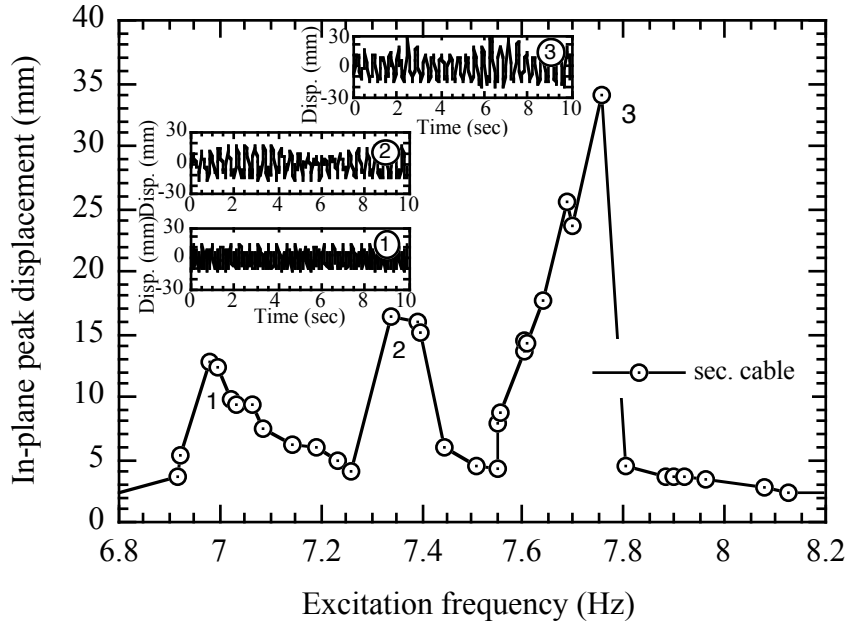

(b) Frequency response curve for secondary cable

Engineering Structures
Yamaguchi, H. and Alauddin, Md.
Figure 6

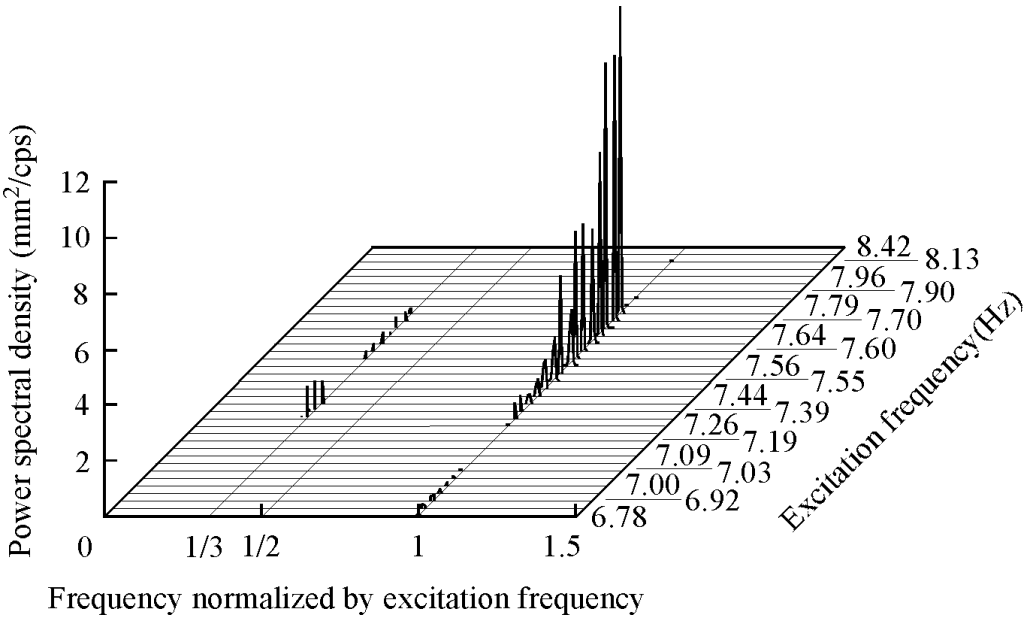

(a) Power spectral density for main cable

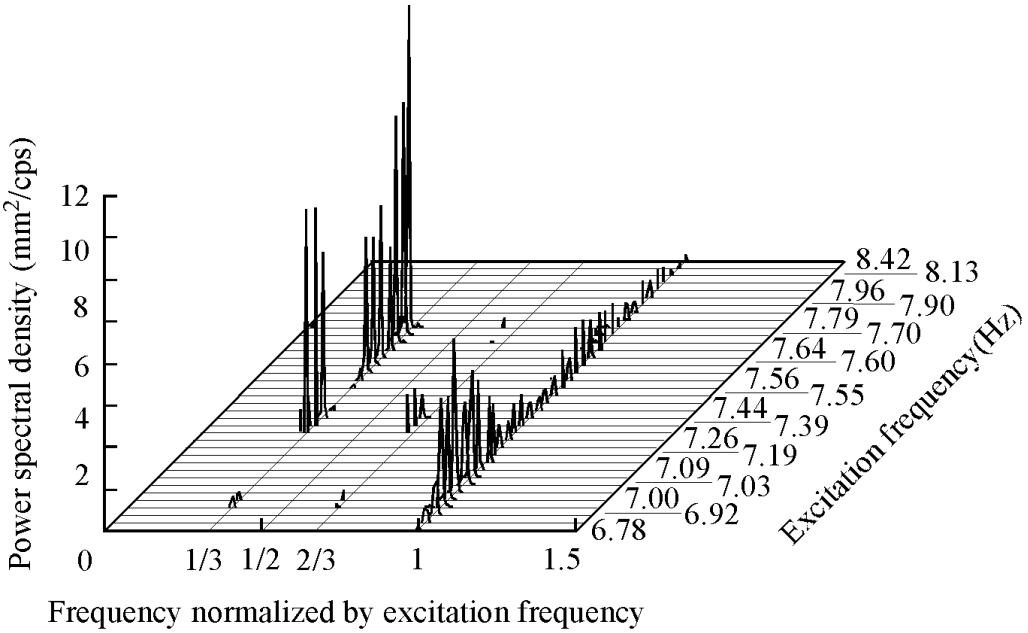

(b) Power spectral density for secondary cable

Engineering Structures
Yamaguchi, H. and Alauddin, Md.
Figure 7

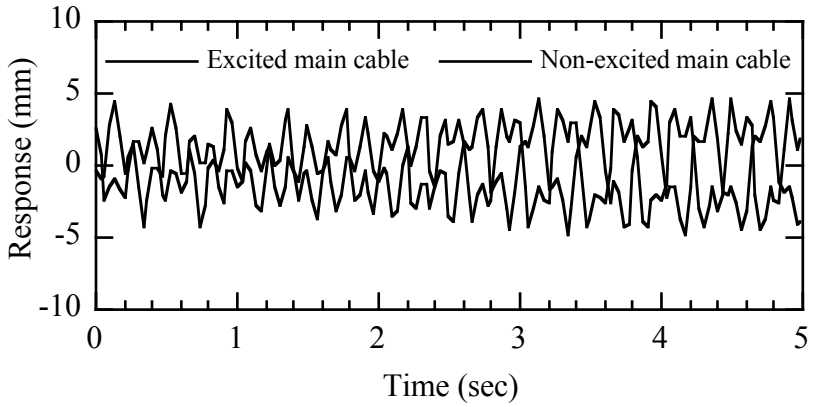

(a) Excitation frequency = 7.34 Hz

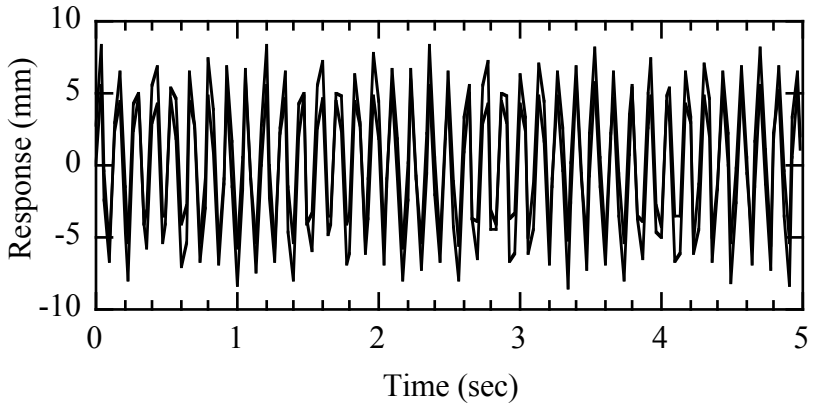

(b) Excitation frequency = 7.70 Hz

Engineering Structures
Yamaguchi, H. and Alauddin, Md.
Figure 8

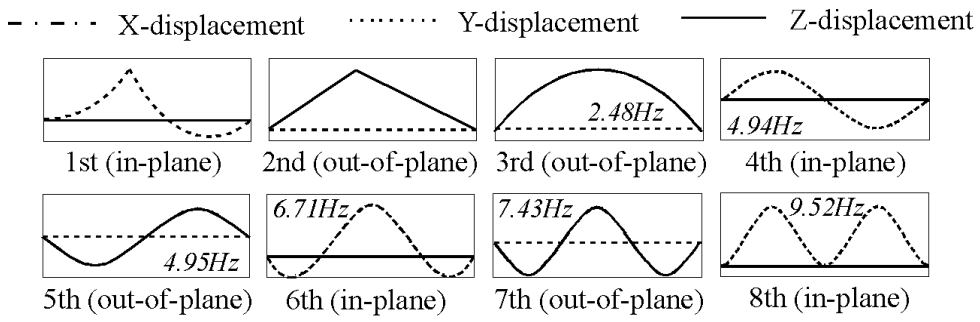

(a) Main cable (1st–2nd: constraint mode, 3rd-8th: normal mode)

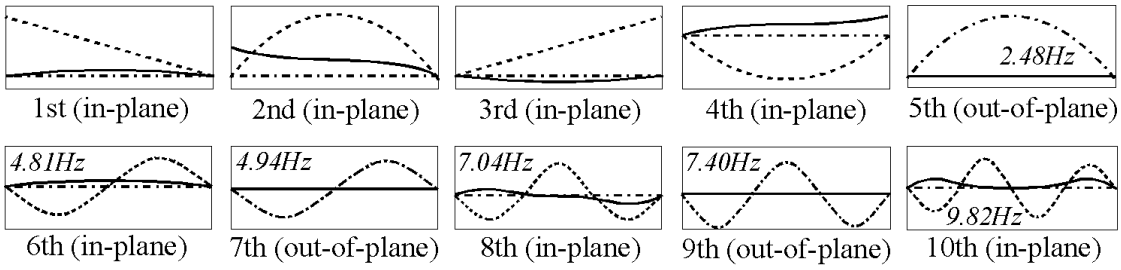

(b) Secondary cable (1st–4th: constraint mode, 5th-10th: normal mode)

Engineering Structures
Yamaguchi, H. and Alauddin, Md.
Figure 9

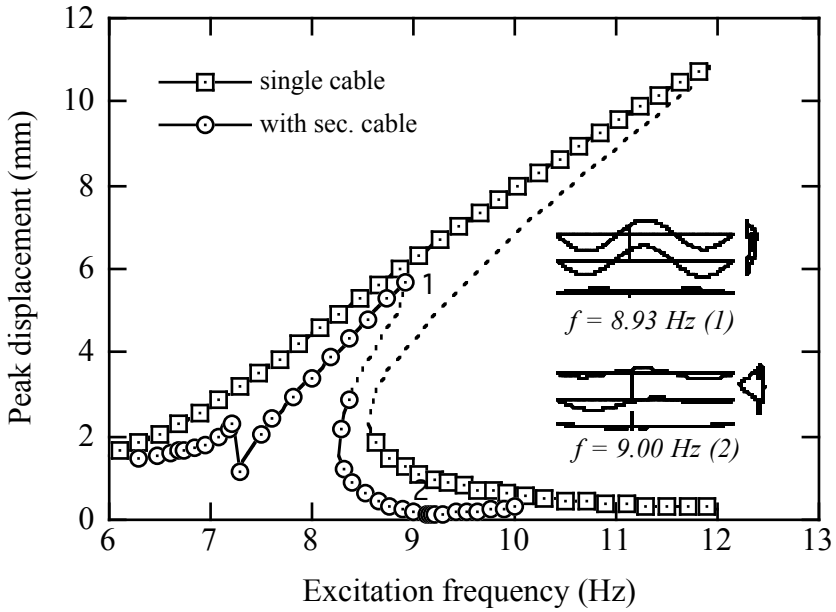

Engineering Structures
Yamaguchi, H. and Alauddin, Md.
Figure 10

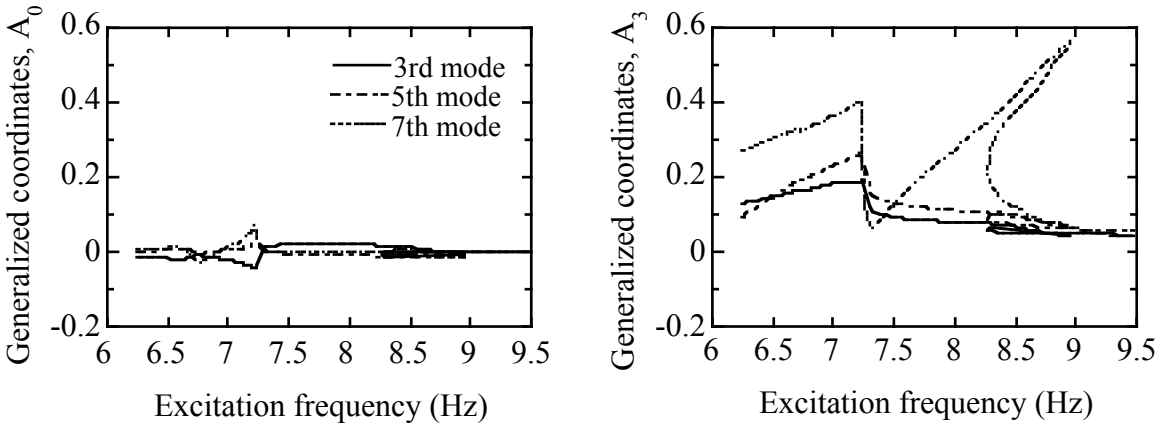

(a) Generalized coordinates, A0 and A3, for the 3rd, 5th and 7th substructural modes (out-of-plane mode) in Fig. 9

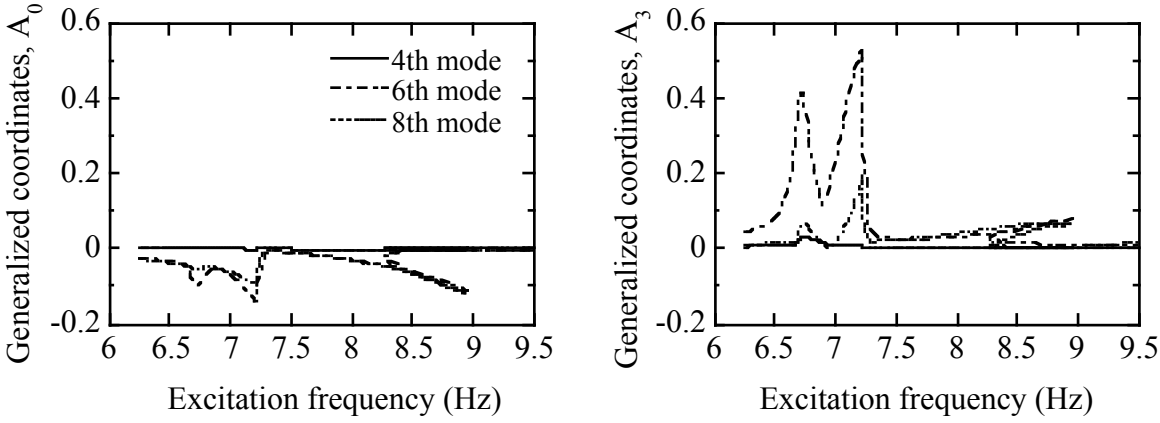

(b) Generalized coordinates, A0 and A3, for the 4th, 6th and 8th substructural modes (in-plane mode) in Fig. 9

Engineering Structures
Yamaguchi, H. and Alauddin, Md.
Figure 11

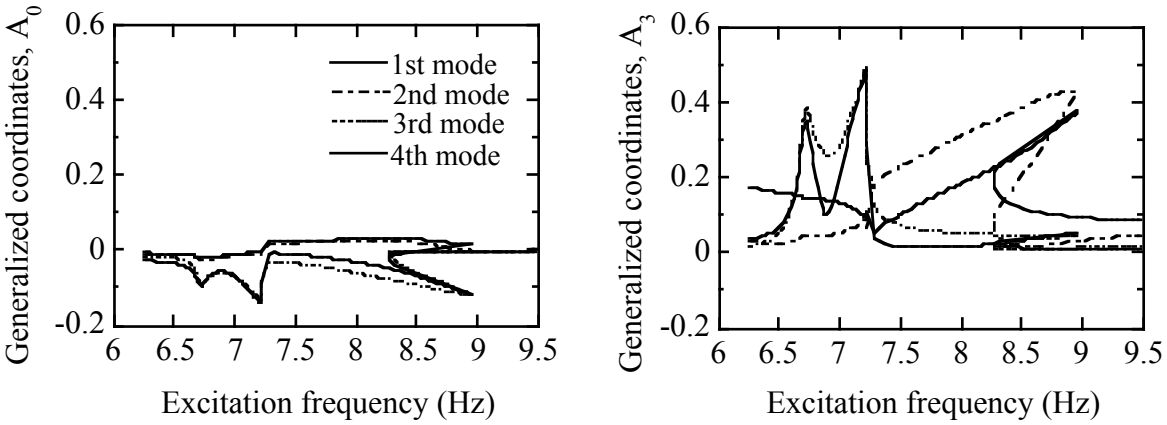

(a) Generalized coordinates, A0 and A3, for the 1st - 4th substructural modes (constraint mode) in Fig. 9

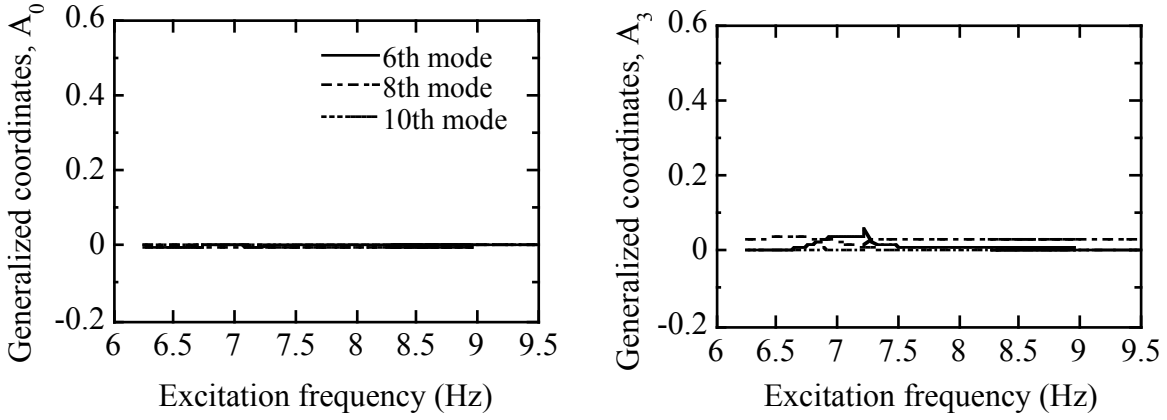

(b) Generalized coordinates, A0 and A3, for the 6th, 8th and 10th substructural modes (normal mode) in Fig. 9

Engineering Structures
Yamaguchi, H. and Alauddin, Md.
Figure 12

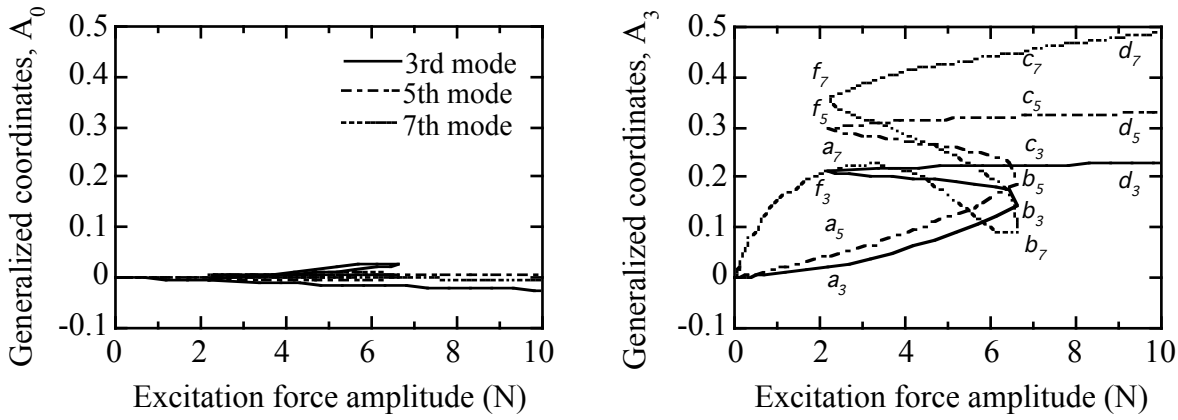

(a) Generalized coordinates, A0 and A3, for the 3rd, 5th and 7th substructural modes (out-of-plane mode) in Fig. 9

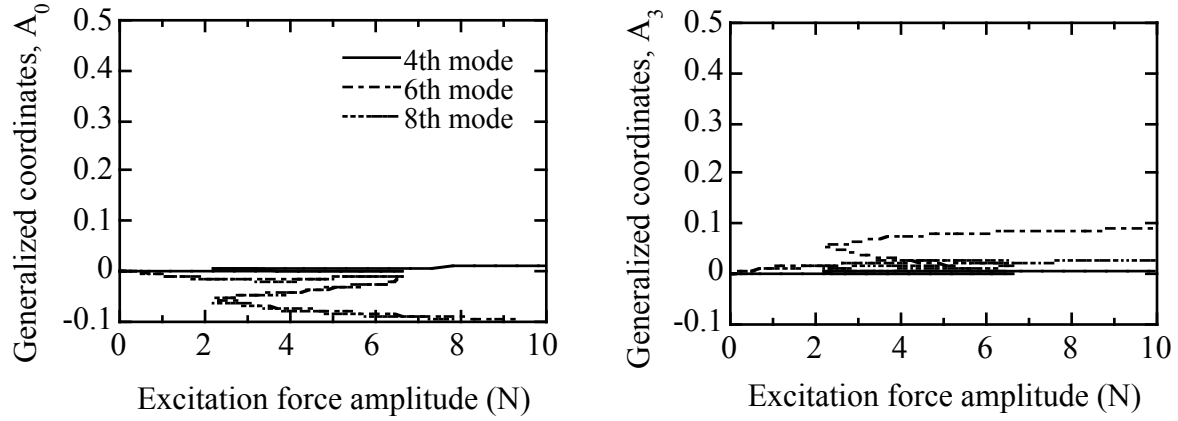

(b) Generalized coordinates, A0 and A3, for the 4th, 6th and 8th substructural modes (in-plane mode) in Fig. 9

Engineering Structures
Yamaguchi, H. and Alauddin, Md.
Figure 13

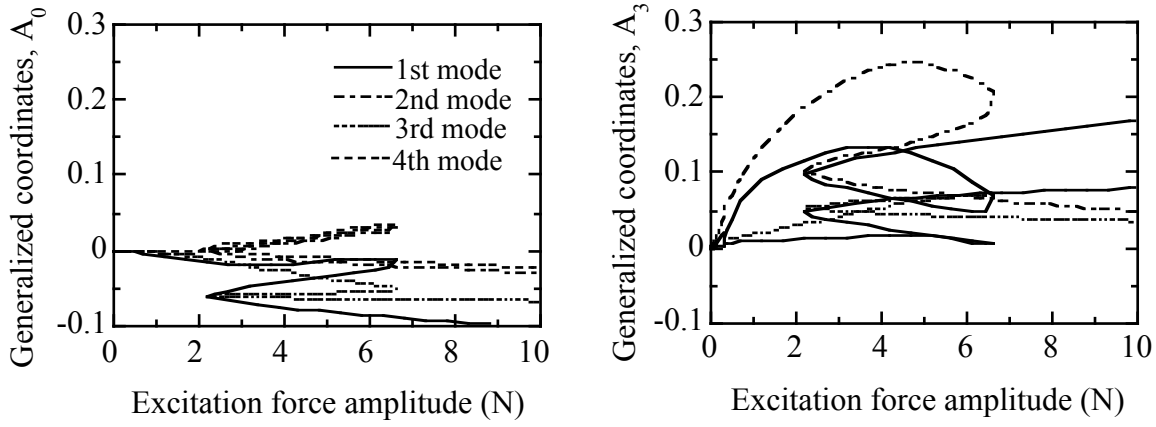

(a) Generalized coordinates, A0 and A3, for the 1st - 4th substructural modes (constraint mode) in Fig. 9

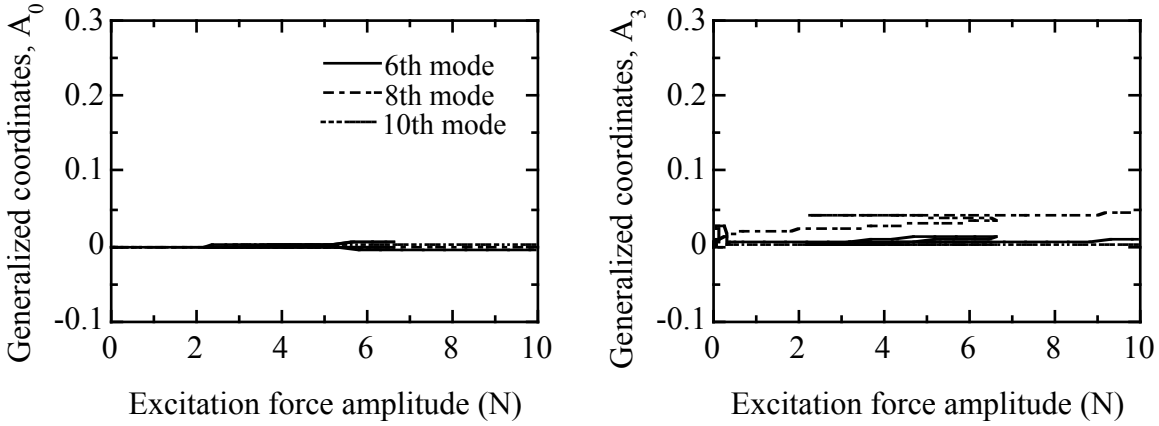

(b) Generalized coordinates, A0 and A3, for the 6th, 8th and 10th substructral modes (normal mode) in Fig. 9

Engineering Structures
Yamaguchi, H. and Alauddin, Md.
Figure 14

(a) P = 2.66 N (b) P = 6.66 N (c) P = 6.84 N

Engineering Structures
Yamaguchi, H. and Alauddin, Md.
Figure 15

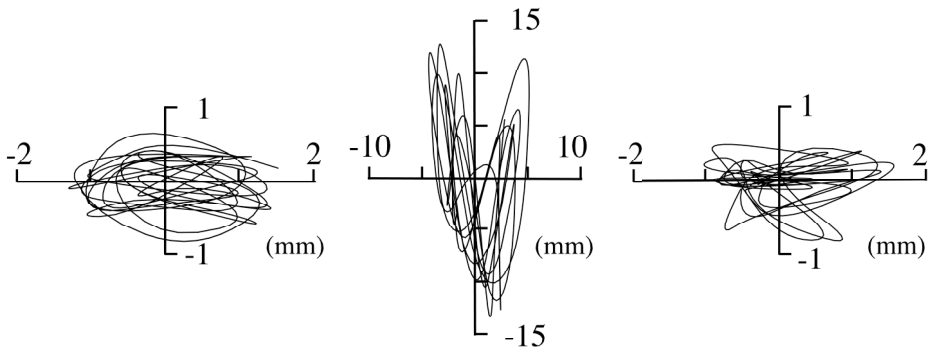

(1) (2) (3)

(a) Excitation frequency = 6.95 Hz

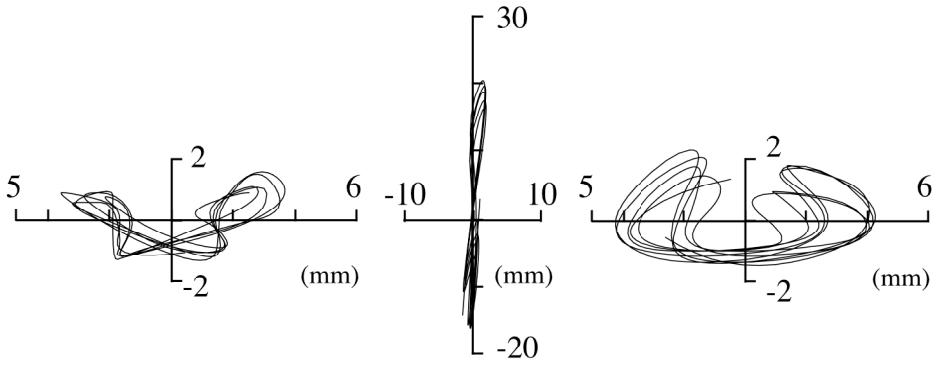

(1) (2) (3)

(b) Excitation frequency = 7.34 Hz

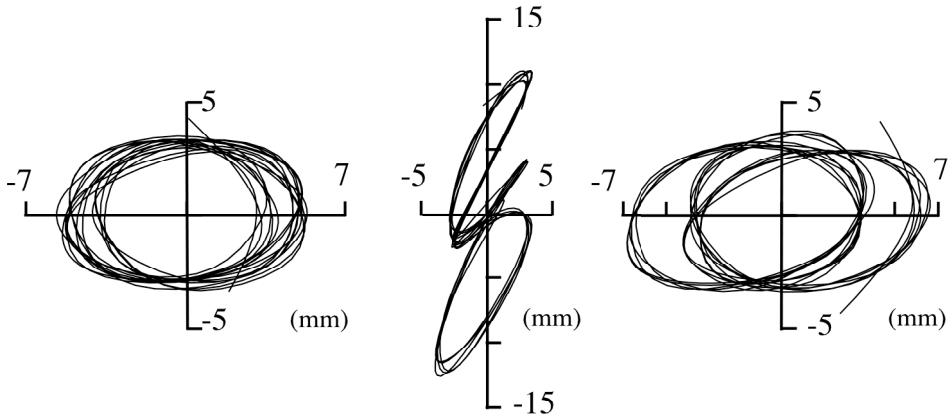

(1) (2) (3)

(c) Excitation frequency = 7.71 Hz

Engineering Structures
Yamaguchi, H. and Alauddin, Md.
Figure B1